

# Theoretical study on interactions of $\beta$ -cyclodextrin with helicobacter pylori eradicating agent (TG44)

Xin Jin · Xueye Wang · Cuihuan Ren · Yuan Miao · Ling Yi

Received: 22 April 2010 / Accepted: 11 June 2010 / Published online: 7 July 2010  
© Springer-Verlag 2010

**Abstract** The inclusion complex of  $\beta$ -cyclodextrin ( $\beta$ -CD) and 4-methylbenzyl-4'-[trans-4-(guanidinomethyl)cylohexylcarbonyloxy]-biphenyl-4-carboxylate monohydrochloride (TG44) had been investigated by using density functional theory (DFT) and PM3 semiempirical method. The results indicate that the  $\beta$ -CD includes predominantly the biphenyl moiety of TG44, and the inclusion complex formed by TG44 entering into the cavity of  $\beta$ -CD from its narrow side (the primary hydroxyl group side) is more stable than that formed by TG44 entering into the cavity of  $\beta$ -CD from its wide side (the secondary hydroxyl group side). The negative enthalpy changes calculated from the statistical thermodynamic calculations at 1 atm and 298.15 K suggest that the inclusion complexes are favored enthalpy-driven processes. The molecular modeling results are in good agreement with the experiment for 2D  $^1\text{H}$ – $^{13}\text{C}$  H HETCOR spectroscopic and H-NMR spectroscopic observations.

**Keywords** Cyclodextrin · Density functional theory (DFT) · Inclusion complex · PM3 · TG44

## Introduction

The study of inclusion complexes of organic molecules with cyclodextrins has attracted the interest of many experimental and theoretical chemists during the past decades [1, 2]. Cyclodextrins are the natural cyclic oligosaccharides consti-

tuted mainly by the six ( $\alpha$ -cyclodextrin,  $\alpha$ -CD), seven ( $\beta$ -cyclodextrin,  $\beta$ -CD) and eight ( $\gamma$ -cyclodextrin,  $\gamma$ -CD) D-glucose units linked in  $\alpha$ -(1→4) (Fig. 1a) [3]. Cyclodextrins are known for their ability to bind organic molecules by non-covalent interactions and it has been reported that the hydrophobic effects, van der Waals interactions, dipole-dipole interactions and charge transfer interactions are the possible driving forces for the inclusion complex [4]. In particular,  $\beta$ -cyclodextrin ( $\beta$ -CD) has an internal cavity shaped like a truncated cone of about 8 Å deep and 6.0–6.4 Å in diameter. This cavity possesses a relatively low polarity, so it can accommodate guest organic molecules inside [5]. By this means,  $\beta$ -CD can improve the stability, dispersing and dissolving properties of some drugs, and enhance its physical and chemical activity through the inclusion complexes [6]. Therefore,  $\beta$ -CD is by far the most widely used in pharmaceutical sciences and different fields of chemistry ranging from analytical to synthetic chemistry in cyclodextrins [7, 8].

4-Methylbenzyl-4'-[trans-4-(guanidinomethyl)cylohexylcarbonyloxy]-biphenyl-4-carboxylate monohydrochloride (TG44, Fig. 1b) is a newly synthesized Helicobacter pylori (H. pylori) eradicating agent with high selectivity to H. pylori, compared with other Gram-negative and Gram-positive bacteria [9, 10]. In recent years, the association between Helicobacter pylori and gastritis, gastric ulceration, and duodenal ulceration, as well as gastric cancer, has been clarified [11, 12]. H. pylori is well recognized as a major etiologic factor for gastritis and peptic ulceration [13, 14] and the eradication of H. pylori drastically reduces the recurrence of ulceration and is considered essential to treat ulceration. However, pharmaceutical applications of TG44 are limited due to its very low solubility in water (0.036±0.004 mM at 25°C) [15]. However, the H. pylori eradicating activity of TG44 is markedly enhanced when it is orally

X. Jin · X. Wang (✉) · C. Ren · Y. Miao · L. Yi  
Key Laboratory of Environmentally Friendly Chemistry  
and Applications of Ministry of Education, College of Chemistry,  
Xiangtan University,  
Xiangtan, Hunan 411105, People's Republic of China  
e-mail: wxueye@xtu.edu.cn

**Fig. 1** Molecular structures of  $\beta$ -CD (a), TG44 (b) and B3LYP/6-31G\* optimized structure of TG44 (c)

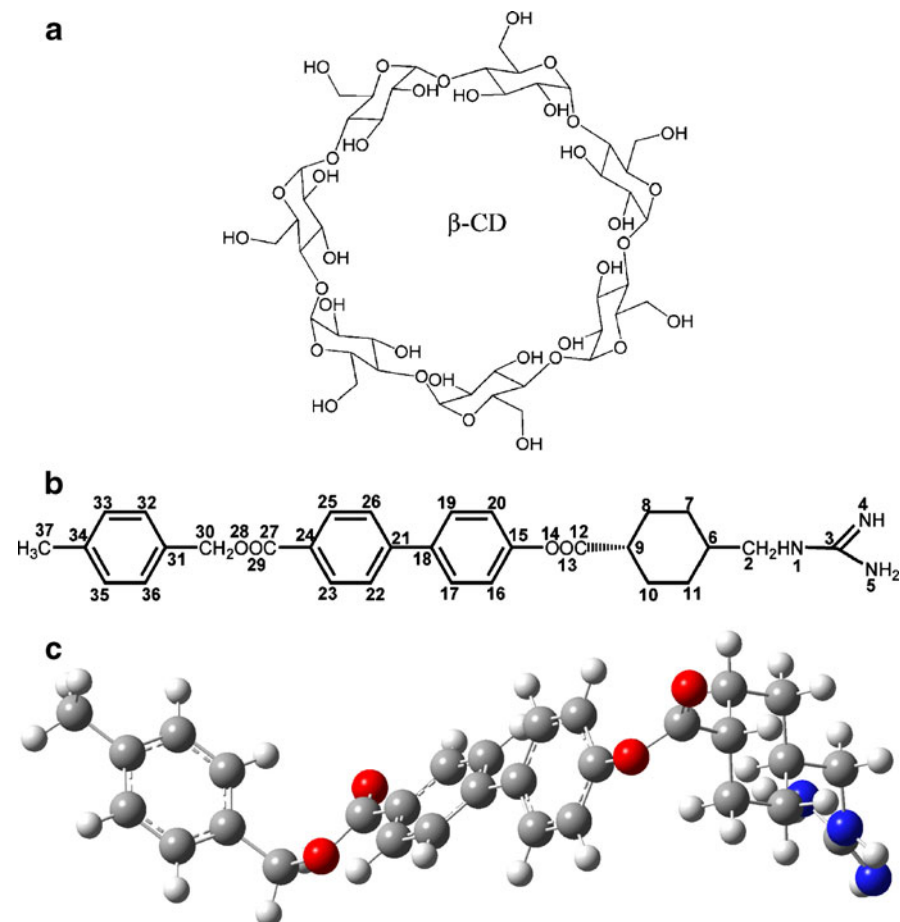


**Fig. 2** Coordinate systems used to define the process of complexation for: (a) head up and (b) head down. Part 1 represents the methylbenzene moiety. Part 2 represents the biphenyl moiety. Part 3 represents the cyclohexane moiety

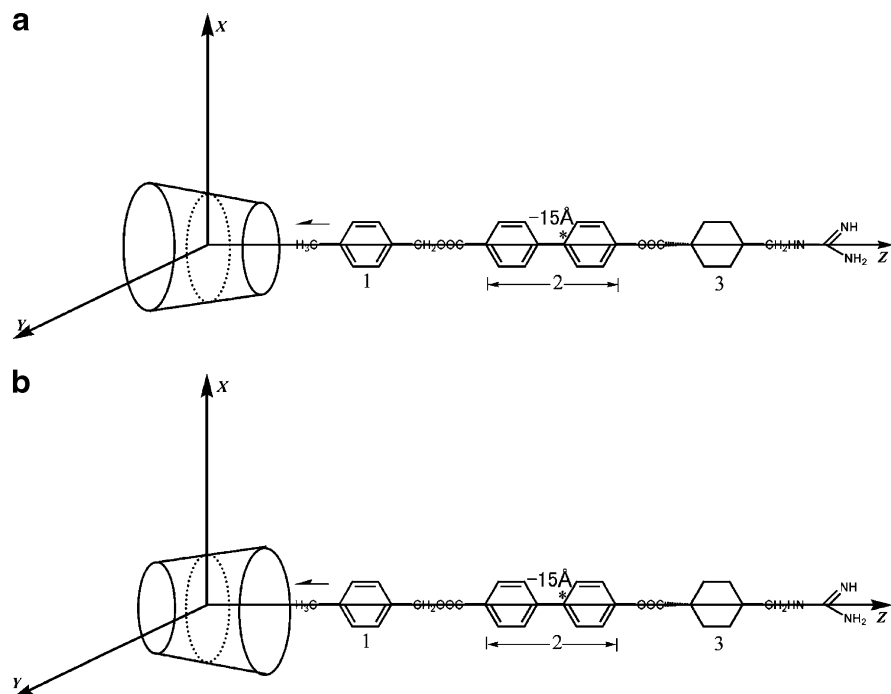


**Table 1** Thermodynamic parameters of the models C and c calculated by PM3 method and the single point energies by B3LYP/6-31G\*

Species PM3	TG44	$\beta$ -CD	Head up	Head down
$E^a(\text{kJ molK}^{-1})$	-384.04	-6085.41	-6551.17	-6548.78
$\Delta E^a(\text{kJ molK}^{-1})$	—	—	-81.72	-79.33
$H_f(\text{kJ molK}^{-1})$	1221.79	-2778.65	-1629.44	-1627.19
$\Delta H^b(\text{kJ molK}^{-1})$	—	—	-72.61	-70.33
$G_f(\text{kJ molK}^{-1})$	929.14	-3279.39	-2334.02	-2333.56
$\Delta G^b(\text{kJ molK}^{-1})$	—	—	16.23	16.69
$\Delta S^\circ(\text{J mol}^{-1} \text{ K}^{-1})$	—	—	-297.97	-291.87
$E_{\text{HOMO}}(\text{eV})$	-9.20	-10.56	-9.28	-9.28
$E_{\text{LUMO}}(\text{eV})$	-1.01	1.09	-1.09	-1.22
$E_{\text{HOMO}} - E_{\text{LUMO}}$ (eV)	-8.19	-11.65	-8.19	-8.06
B3LYP/6-31G*				
$E^a(\text{kJ molK}^{-1})$	-4274999.02	-11224644.99	-15499659.14	-15499635.42
$\Delta E^a(\text{kJ molK}^{-1})$	—	—	-15.13	8.59

<sup>a</sup>  $E$  is the HF energy,  $\Delta E$  is the stabilization energy of complexes;

<sup>b</sup>  $\Delta A = A_{\text{complex}} - (A_{\text{subst}} + A_{\beta\text{-CD}})$ ,  $A = H, G$ ;

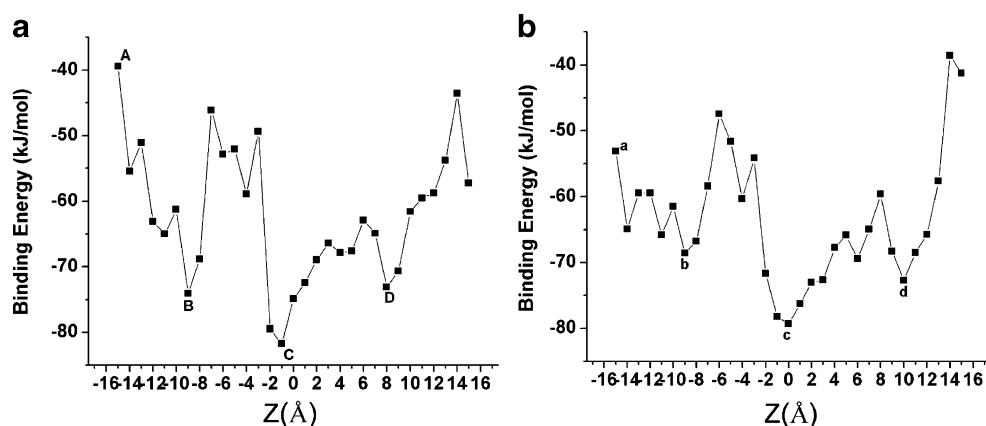
<sup>c</sup>  $\Delta S = (\Delta H - \Delta G)/T$

administered in the form of  $\beta$ -CD complex, compared with TG44 alone. The enhanced antimicrobial activity of TG44/ $\beta$ -CD complex may be ascribed to improved dissolving properties of the  $\beta$ -CD complex. However, due to the limitations of the experimental methods, the geometrical structure and stability of the complex as well as the inclusion energetics of the formation process between the guest molecule and the  $\beta$ -CD host are still not reported yet. Therefore, the molecular modeling methods of cyclodextrins complexes are powerful tools for the understanding of the geometry and the interaction energy of the inclusion compounds.

However, the use of traditional molecular modeling techniques for the study of cyclodextrins is somewhat limited due to the size and flexibility of some molecules, which represent a real challenge for computational methods [16]. As a result, the extensive progress has been made in the use of molecular mechanics (MM) and molecular dynamics (MD) techniques for the study on cyclodextrins and their inclusion complexes [17–19]. However, these methods lack a representation of electron density, missing

many chemically important quantum based effects in spite of they have the advantage of being less resource demanding [20, 21]. In recent years, the quantum chemical calculations of the semiempirical level have become affordable for the study of cyclodextrins and their inclusion complexes. Semiempirical methods employ approximations that accelerate the solution of the Roothan-Hall equations. Thus, they improve the description of quantum phenomena over MM techniques [22]. However, the precision of semiempirical methods is limited since they are parametrized to reproduce experimental observables for a large number of molecules. Moreover, semiempirical methods can fail when treating systems that are not considered in the initial parametrization procedure. Diverse semiempirical methods, such as CNDO [23, 24], AM1 [25], and PM3 [26], have been employed in the study of cyclodextrins and their inclusion compounds. Since 1995, several authors have employed AM1 and PM3 techniques in the study of cyclodextrins. The work of Bodor [27] have been studied in detail about the performances of AM1. The work of Avakyan [28] and Liu [29–33] has proved that PM3 has a

**Fig. 3** Stability energies of the inclusion complexation of TG44 into  $\beta$ -CD at different positions (Z) and models: (a) head up; (b) head down. Point A, B, C, D represent  $Z_A = -15 \text{ \AA}$ ,  $Z_B = -9 \text{ \AA}$ ,  $Z_C = -1 \text{ \AA}$ ,  $Z_D = 8 \text{ \AA}$ , respectively. Point a, b, c, d represent  $Z_a = -15 \text{ \AA}$ ,  $Z_b = -9 \text{ \AA}$ ,  $Z_c = 0 \text{ \AA}$ ,  $Z_d = 10 \text{ \AA}$  respectively



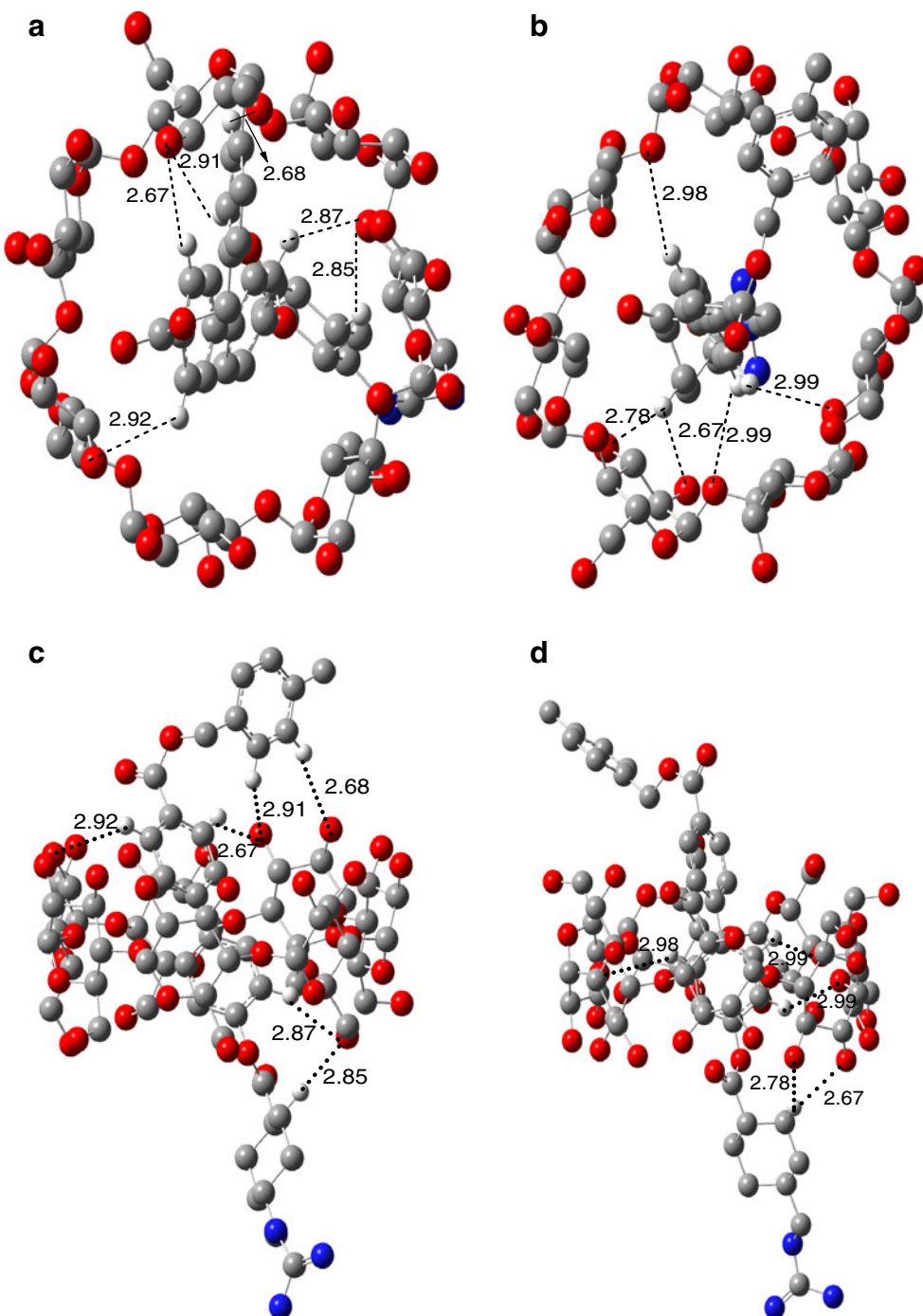
better performance in the cyclodextrin geometry optimization since it can deal with intramolecular hydrogen bonds.

## Computational methods

The inclusion model can be seen in Fig. 2. It contains one passing process and one circling process. The glycosidic

oxygen atoms of  $\beta$ -CD are placed in XY plane and their center is defined as the center of the whole system. TG44 approaches and passes through the cavity of  $\beta$ -CD from + Z to – Z direction, and the distance between the labeled carbon atom C\* (symmetric center of TG44) and  $\beta$ -CD ranges from -15 to +15 Å. The guest is initially located at a Z-coordinate of 15 Å and is moved through the host cavity along the Z-axis to -15 Å with a stepwise 1 Å. For each

**Fig. 4** Structures of the inclusion models C and c optimized by the PM3 method. The inclusion complexes are formed by TG44 entering into the cavity of  $\beta$ -CD from its narrow side (the primary hydroxyl group side) (a, c) and wide side (the secondary hydroxyl group side) (b, d). Fig (a) and (c) are the top and side view of model C, respectively. Fig (b) and (d) are top and side view of model c, respectively. Dotted lines are the H-bonds length (Å) between TG44 and  $\beta$ -CD. Gray balls represent the carbon atoms, red balls represent oxygen atoms, white balls represent hydrogen atoms



step, the geometry of the complex is fully optimized by PM3 without imposing any symmetrical restrictions. In order to find an even more stable structure of the complex, each guest molecule is calculated for all of the structures obtained by scanning  $\theta$ , clockwise circling around Z-axis, at 30° intervals from 0° to 360°. Stabilization energy upon complexes between TG44 and the  $\beta$ -CD is calculated for the minimum energy structure according to  $\Delta E = E_{\text{compl}} - (E_{\text{subst}} + E_{\beta\text{-CD}})$ .  $E_{\text{compl}}$ ,  $E_{\text{subst}}$  and  $E_{\beta\text{-CD}}$  represent HF energies (heats of formation) of the complex, the free substrate and the free  $\beta$ -CD, respectively. The magnitude of the energy change would be a sign of the driving force toward complexes.

The initial structure of  $\beta$ -CD is built with CS Chem3D Ultra (Version 8.0) from the crystal structure [34] and fully optimized by PM3 method without imposing any symmetrical restrictions. Frequency calculations using PM3 are performed to confirm the completeness of optimization, and no negative eigenvalue was found for the final structures. The density functional theory (DFT) at the level of B3LYP/6-31G\*, which considers the electron correlation and high precision of energy calculations [35, 36], is applied to calculate the single point energies of the inclusion complexes. All the calculations are performed with the Gaussian03 software package [37].

## Results and discussion

### Passing process

All the optimized structures obtained by scanning the  $\theta$  angle, from 0 to 360° at 30° intervals, and the coordinate Z, from -15 to +15 Å at 1 Å intervals, were used to find the

most favorable approach of the TG44/ $\beta$ -CD. Two  $\Delta E$  minima are found at Z=-1 Å,  $\theta=150^\circ$  and Z=0 Å,  $\theta=330^\circ$  for head up model (TG44 entering into the cavity of  $\beta$ -CD from its narrow side, defined as model C) and head down model (TG44 entering into the cavity of  $\beta$ -CD from its wide side, defined as model c). The models are shown in Fig. 2. The negative  $\Delta E$  changes demonstrate that  $\beta$ -CD can form a stable complex with TG44, and the changes are similar to the reports for MM studies on cyclodextrin systems [38]. The thermodynamic parameters are listed in Table 1, the single point energy of model C (-15.13 kJmol<sup>-1</sup>) is 23.72 kJmol<sup>-1</sup> lower than that of model c (8.59 kJmol<sup>-1</sup>) and the PM3 binding energy (-81.72 kJmol<sup>-1</sup>) of model C is also 2.39 kJmol<sup>-1</sup> lower than that of model c (-79.33 kJmol<sup>-1</sup>). This suggests that model C is more stable than model c, and the results predict that the TG44 molecule prefers to enter the cavity of  $\beta$ -CD from its narrow side rather than the wide side. Besides, The gap ( $E_{\text{LUMO}}-E_{\text{HOMO}}$ ) is an important stability index [39], and chemicals with larger ( $E_{\text{LUMO}}-E_{\text{HOMO}}$ ) values tend to have higher stability, therefore, the head up model is significantly more favorable than the head down model by ( $E_{\text{LUMO}}-E_{\text{HOMO}}$ ) values.

The energy changes of TG44/ $\beta$ -CD<sub>head-up</sub> and TG44/ $\beta$ -CD<sub>head-down</sub> in the passing process are shown in Fig. 3a, b, respectively. As shown in Fig. 3a (the methylbenzene moiety entering from narrow primary hydroxyl sides of the cavity), the energy decreases by 34.696 kJmol<sup>-1</sup> from the starting point A (Z<sub>A</sub>=-15 Å, Z<sub>A</sub> is the Z-coordinate of point A) to point B (Z<sub>B</sub>=-9 Å). Then, the energy increases sharply, and rapidly drops down to the point C (Z<sub>C</sub>=-1 Å). Finally, the energy increases slowly, and drops down to the point D (Z<sub>D</sub>=8 Å) suddenly through a certain degree of perturbation. When the TG44 molecule enters into the cavity of  $\beta$ -CD from the wide side, the energy curve

**Fig. 5** PM3 optimized structure of  $\beta$ -CD (a) and structure of  $\beta$ -CD after guest inclusion (b). Fig (b) is model C after removal of the structure of the TG44. The solid lines length represent the distance between numbered atoms. H-bonds are formed between underlined atoms O-106, O-96, O-92 and the TG44. The glycosidic oxygen atoms of  $\beta$ -CD number are O-97, O-102, O-107, O-113, O-118, O-122, O-126. Gray balls represent the carbon atoms, red balls represent oxygen atoms

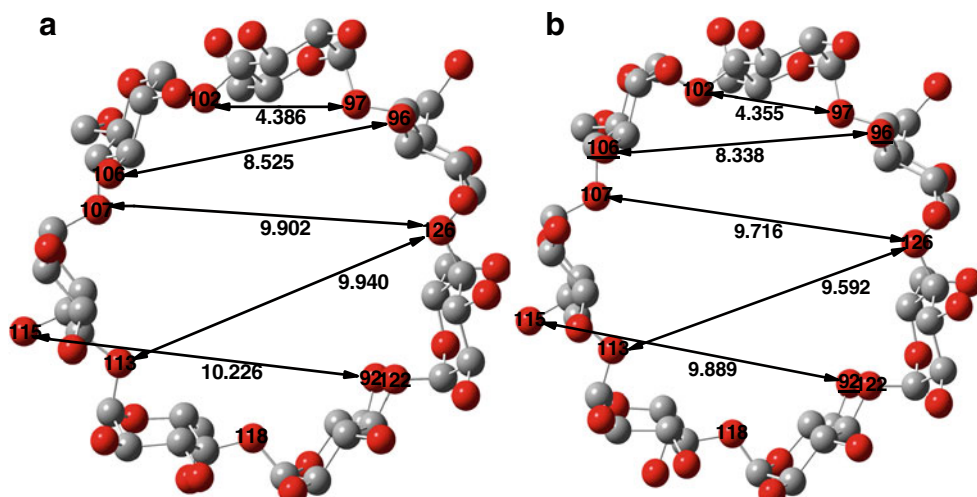


(Fig. 3b) is somewhat similar to the process entering from the narrow side. Points a, b, c, d appear in  $Z_a = -15 \text{ \AA}$ ,  $Z_b = -9 \text{ \AA}$ ,  $Z_c = 0 \text{ \AA}$ ,  $Z_d = 10 \text{ \AA}$  respectively. Obviously, point C and c are the global minimum of the whole curve, the curves indicate that TG44 and  $\beta$ -CD could form the most stable complexes. In these two positions ( $Z_C = -1 \text{ \AA}$  and  $Z_c = 0 \text{ \AA}$ ), the biphenyl moiety of TG44 just full access to the

central of  $\beta$ -CD cavity. This is in a good agreement with the conclusion of the solid NMR spectroscopic experiment [6], in which the  $\beta$ -CD includes predominantly the biphenyl moiety of TG44. Besides, the methylbenzene moiety full access to central of  $\beta$ -CD cavity at point B and b ( $Z_B = -9 \text{ \AA}$   $Z_b = -9 \text{ \AA}$ ) and the cyclohexane moiety full access to central of  $\beta$ -CD cavity near the point D and d ( $Z_D = 8 \text{ \AA}$ ,  $Z_d = 10 \text{ \AA}$ ).

**Table 2** Mulliken charges(e) of the heavy atoms of TG44, charge transfer of the two models calculated by B3LYP/6-31G\* and PM3 methods

Atoms	TG44		Head up		Head down	
	PM3	B3LYP/6-31G*	PM3	B3LYP/6-31G*	PM3	B3LYP/6-31G*
N <sub>1</sub>	0.0632	-0.2741	0.0663	-0.2716	0.0637	-0.2751
C <sub>2</sub>	0.0252	0.1691	0.0232	0.1659	0.0262	0.1727
C <sub>3</sub>	-0.0925	0.5211	-0.0915	0.5214	-0.0911	0.5228
N <sub>4</sub>	-0.1265	-0.3503	-0.1295	-0.3525	-0.1301	-0.3518
N <sub>5</sub>	0.1239	-0.0812	0.1214	-0.0844	0.1261	-0.0788
C <sub>6</sub>	-0.0126	0.0154	-0.0116	0.0151	-0.0072	0.0209
C <sub>7</sub>	0.0194	0.0093	0.0160	0.0074	0.0157	0.0134
C <sub>8</sub>	0.0248	0.0304	0.0331	0.0358	0.0334	0.0313
C <sub>9</sub>	0.0079	-0.0064	0.0254	-0.0112	0.0150	-0.0058
C <sub>10</sub>	0.0220	0.0193	0.0285	0.0277	0.0303	0.0119
C <sub>11</sub>	0.0208	0.0139	0.0173	0.0117	0.0222	0.0214
C <sub>12</sub>	0.3546	0.5508	0.3882	0.6246	0.3949	0.6127
O <sub>13</sub>	-0.3304	-0.4438	-0.3681	-0.477	-0.4005	-0.491
O <sub>14</sub>	-0.1826	-0.4823	-0.2169	-0.5351	-0.2043	-0.5192
C <sub>15</sub>	0.0582	0.2955	0.1033	0.3415	0.0760	0.3022
C <sub>16</sub>	-0.0117	-0.0098	-0.0070	-0.0386	0.0115	0.0066
C <sub>17</sub>	0.0358	-0.0267	0.0337	-0.0142	0.0493	-0.0057
C <sub>18</sub>	-0.0451	0.0868	-0.0679	0.0674	-0.0431	0.0421
C <sub>19</sub>	0.0345	-0.0203	0.0442	-0.0323	0.0294	-0.0339
C <sub>20</sub>	0.0126	-0.0052	0.0179	0.0426	-0.0092	0.0135
C <sub>21</sub>	-0.0022	0.0908	0.0149	0.0934	-0.0173	0.0552
C <sub>22</sub>	-0.0017	-0.0303	-0.0022	-0.0129	0.0200	0.0072
C <sub>23</sub>	0.0748	0.0036	0.0513	-0.0389	0.0551	0.0065
C <sub>24</sub>	-0.1229	0.0617	-0.1531	0.0124	-0.1384	0.0230
C <sub>25</sub>	0.0753	0.0030	0.0584	0.0036	0.0718	0.0151
C <sub>26</sub>	-0.0011	-0.0297	0.0189	-0.0057	0.0062	-0.0181
C <sub>27</sub>	0.4273	0.5369	0.4175	0.5069	0.4021	0.4887
O <sub>28</sub>	-0.3790	-0.4783	-0.362	-0.4532	-0.3238	-0.4266
O <sub>29</sub>	-0.2627	-0.4661	-0.2219	-0.4064	-0.2284	-0.4166
C <sub>30</sub>	0.2464	0.2099	0.2115	0.1733	0.1829	0.1638
C <sub>31</sub>	-0.1435	0.0973	-0.1276	0.1238	-0.1166	0.1087
C <sub>32</sub>	0.0336	-0.0283	0.0207	-0.0303	0.0399	-0.0115
C <sub>33</sub>	-0.0072	-0.0406	-0.0033	-0.0540	-0.0008	-0.0393
C <sub>34</sub>	-0.0618	0.1298	-0.0553	0.1265	-0.0629	0.1324
C <sub>35</sub>	-0.0026	-0.0386	0.0030	-0.0304	-0.0002	-0.0404
C <sub>36</sub>	0.0523	-0.0031	0.0448	-0.0188	0.0411	-0.0187
C <sub>37</sub>	0.0734	-0.0293	0.0774	-0.0177	0.0719	-0.0327
Charge	-0.0000	0.0000	0.0189	0.0159	0.0106	0.0068
transfer						

Based on the above energy analysis, the most stable structure is model C. A similar conclusion is obtained by H-NMR experiment [15].

- (1). Geometrical structure The PM3-optimized structures of models C and c are shown in Fig. 4, there are several intermolecular H-bonds in the structures. Here, the H-bond is defined as C-H···O or O-H···O and the C-H···O H-bond length shorter than 3.0 Å which just falls in the reported data [40]. In order to observe the H-bonds more clearly, the extra hydrogen atoms have been omitted. Obviously, the hydrogen bonds of model c are less than that of model C. This explains why the binding energy of the inclusion model C is 2.394 kJmol<sup>-1</sup> lower than that of model c. The calculated results are in a good agreement with the peak of ROESY spectrum experiments [15] in head up model. Unexpectedly, the optimized geometries reveal that there is no O-H···O H-bond interactions between  $\beta$ -CD and the TG44 because the [O···O] distance shorter than 2.5 Å which just falls in the reported data [41, 42]. Besides, the geometrical changes of  $\beta$ -CD after guest inclusion are shown in Fig. 5. We found that solid lines length in Fig. 5b are shorter than Fig. 5a. As H-bonds are formed between underlined atoms O-106, O-96, O-92 and the TG44, the round cavity of  $\beta$ -CD turns into an oval-shaped cavity. Atoms O-106 and O-96 are part of the hydroxyl groups of the top rim of  $\beta$ -CD. Atom O-92 is the part of the hydroxyl groups of bottom rim of  $\beta$ -CD. Therefore, the hydroxyl groups of the top/bottom rim of  $\beta$ -CD play a significant role in binding the TG44.
- (2). Charge transfer Liu and Guo suggest that charge transfer interactions play a relevant role in the stabilization of their inclusion complexes [43]. The Mulliken charges of the heavy atoms of TG44, charge transfer of the models are summarized in Table 2 by B3LYP/6-31G\* and PM3 methods. The data show that

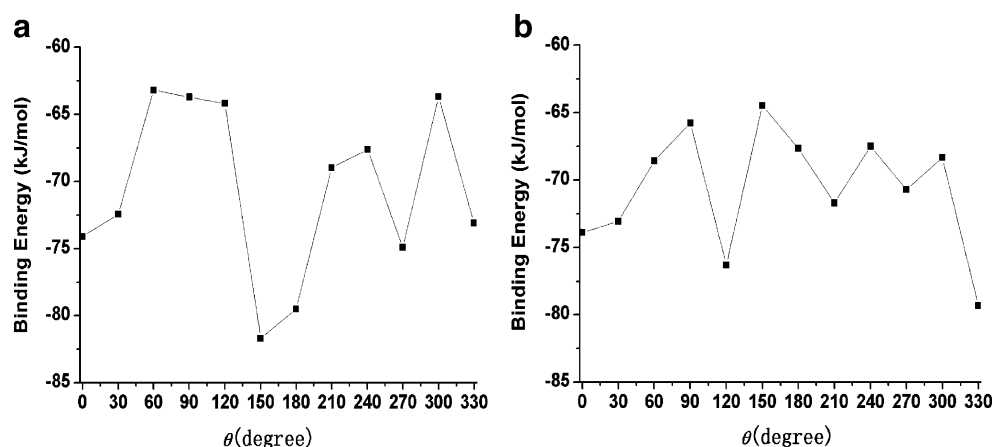
the  $\beta$ -CD molecule accepts the electron from TG44, and the charge transfer of TG44 head up model (PM3: 0.0189e, B3LYP/6-31G\*:0.0159e) is larger than head down model (PM3: 0.0106e, B3LYP/6-31G\*:0.0068e).

- (3). Thermodynamic analysis To investigate the thermodynamics of the binding process, the statistical thermodynamic calculation were carried out at 1 atm and 298.15 K by PM3. The thermodynamic quantities, the enthalpy change ( $\Delta H$ ), the thermal Gibbs free energy ( $\Delta G$ ) and entropy contribution ( $\Delta S$ ) are given in Table 1. The complex reactions of TG44 with  $\beta$ -CD are exothermic judged from the negative enthalpy changes. And the negative enthalpy changes suggest that both the inclusion processes are enthalpically favorable in nature. On the other hand, the enthalpy change for the head up model is more negative than that for the head down model, which is surely attributed to the more tightly van der Waals interactions. In addition, it can be seen that the entropy change ( $\Delta S$ ) of model C and c are also both negative, this indicates that the formation of the complex becomes an enthalpy-driven process. Certainly, since the inclusion reactions happen in aqueous solution, the influence of water molecules on the inclusion process should be very important. However, because of the limitation of our computer, it can hardly calculate the interactions of cyclodextrins systems in aqueous solution. Therefore, the values of thermodynamics calculated has no absolute meaning.

### Circling process

The most stable initial structures studied in circling process are the models C and c. TG44 is placed in XY plane and circled clockwise around the Z-axis from 0° to 360° at 30° intervals. The energy changes of head up and head down are shown in Fig. 6. The energy undulates in a certain scope

**Fig. 6** Stability energies of the inclusion complex for TG44/ $\beta$ -CD at different scanning  $\theta$ , head up (a) and head down (b)



which ranges from 0 to 18.06 kJmol<sup>-1</sup> for head up and 0 to 14.84 kJmol<sup>-1</sup> for head down, respectively. The purpose of the circling process is to improve the accuracy of the lowest energy and most stable structure at each step [33]. Theoretically, the whole potential energy surface can be scanned and the global minimum can be identified when the angle of rotation is reduced at each step. But as the computer restrictions, 30° intervals may be more reasonable.

## Conclusions

The stable structures and the inclusion process for *TG44/β-CD* inclusion complexes were studied by use of quantum mechanics DFT and PM3 methods. The  $\beta$ -CD includes predominantly the biphenyl moiety of *TG44*, and the inclusion complex formed by *TG44* entering into the cavity of  $\beta$ -CD from its narrow side (the primary hydroxyl group side) is more stable than that formed by *TG44* entering into the cavity of  $\beta$ -CD from its wide side (the secondary hydroxyl group side). In addition, the statistical thermodynamic calculations suggest that the formation of the inclusion complex is an enthalpy-driven process. The calculations on the complexes of  $\beta$ -CD with *TG44* support the experimental results of 2D  $^1\text{H}$ – $^{13}\text{C}$  H HETCOR spectroscopic and H-NMR spectroscopic.

**Acknowledgments** The authors wish to acknowledge the financial supports from the Scientific Research Fund of Hunan Provincial Education Department (No. 09A091) for the research work.

## References

- Szejtli J (1998) Chem Rev 98:1743–1754
- Uekama K, Hirayama F, Irie T (1998) Chem Rev 98:2045–2076
- Bender ML, Komiyama M (1978) Cyclodextrin Chemistry. Springer, Berlin
- Rafati AA, Hashemianzadeh SM, Nojini ZB, Safarpour MA (2007) J Mol Liq 135:153–157
- Vögtle F (1991) Supramolecular Chemistry. Wiley, New York
- Anzai K, Kono H, Mizoguchi J, Yanagi T, Hirayama F, Arima H, Uekama K (2006) Carbohydr Res 341:499–506
- Saenger W (1980) Angew Chem 19:344–362
- Szejtli J (1988) Cyclodextrins Technology. Kluwer, Dordrecht
- Dore P, Osato MS, Realdi G, Mura I, Graham DY, Sepulvede AR (1999) J Antimicrob Chemother 43:47–54
- Ossenkopp YJ, Herscheid AJ, Pot RGJ, Kuipers EJ, Kusters JG, Vandebroucke-Grauls CMJE (1999) J Antimicrob Chemother 43:511–515
- El-Omar EM, Carrington M, Chow WH, McColl KEL, Bream JH, Young HA, Herrera J, Lissowska J, Yuan CC, Rothman N, Lanyon G, Martin M, Faumeni JF, Rabkin CS (2000) Nature 404:398–402
- Webb PM, Forman D (1995) Bailliere's Clin Gastroenterol 9:563–582
- Labenz J, Börsch G (1994) Gut 35:19–22
- Nomura A, Stemmermann GN, Chyou PH, Perez-Perez GI, Blaser MJ (1994) Ann Intern Med 120:977–981
- Anzai K, Mizoguchi J, Yanagi T, Hirayama F, Arima H, Uekama K (2007) Chem Pharm Bull 55:1466–1470
- Lipkowitz KB (1998) Chem Rev 98:1829–1873
- Kozár T, Venanzi CA (1997) J Mol Struct 395:451–468
- Fathallah M, Fotiadu F, Jaime C (1994) J Org Chem 59:1288–1293
- Bonnet P, Jaime C, Morin-Allory L (2002) J Org Chem 67:8602–8609
- Jagielska A, Arnautova YA, Scheraga HA (2004) J Phys Chem B 108:12181
- Cramer CJ (2002) Essentials of Computational Chemistry Theories and Models. John Wiley & Sons Ltd, New York
- Jensen F (1999) Introduction to Computational Chemistry. Wiley, New York
- Pople J, Segal GJ (1966) Chem Phys 44:3289–3296
- Sakurai M, Kitagawa M, Hoshi H, Inoue Y, Chūjō R (1990) Carbohydr Res 198:181–191
- Dewar MJS, Zoebisch EG, Healy EF (1985) J Am Chem Soc 107:3902–3909
- Stewart JJP (1989) J Comput Chem 10:209–220
- Bodor N, Huang MJ, Watts JD (1995) J Pharm Sci 84:330–336
- Avakyan VG, Nazarov VB, Alfimov MV, Bagatur'yants AA (1999) Russ Chem Bull 48:1833–1844
- Liu L, Li XS, Song KS, Guo QX (2000) J Mol Struct 531:127–134
- Liu L, Li XS, Guo QX (2000) J Mol Struct 530:31–37
- Liu L, Li XS, Guo QX, Liu YC (1999) Chin Chem Lett 10:1053–1056
- Li XS, Liu L, Guo QX, Chu SD, Liu YC (1999) Chem Phys Lett 307:117–120
- Liu L, Guo X (2004) J Incl Phenom Macrocycl Chem 50:95–103
- Steiner T, Koellner G (1994) J Am Chem Soc 116:5122–5128
- Liu L, Li XS, Mu TW, Guo QX (2000) Monatsh Chem 131:849–855
- Hehre WJ, Ditchfield R, Pople JA (1972) J Chem Phys 56:2257–2261
- Frisch MJ, Trucks GW, Schlegel HB, Scuseria GE, Robb MA, Cheeseman JR, Montgomery JA Jr, Vreven T, Kudin KN, Burant JC, Millam JM, Iyengar SS, Tomasi J, Barone V, Mennucci B, Cossi M, Scalmani G, Rega N, Petersson GA, Nakatsuji H, Hada M, Ehara M, Toyota K, Fukuda R, Hasegawa J, Ishida M, Nakajima T, Honda Y, Kitao O, Nakai H, Klene M, Li X, Knox JE, Hratchian HP, Cross JB, Bakken V, Adamo C, Jaramillo J, Gomperts R, Stratmann RE, Yazyev O, Austin AJ, Cammi R, Pomelli C, Ochterski JW, Ayala PY, Morokuma K, Voth GA, Salvador P, Dannenberg JJ, Zakrewski VG, Dapprich S, Daniels AD, Strain MC, Farkas O, Malick DK, Rabuck AD, Raghavachari K, Foresman JB, Ortiz JV, Cui Q, Baboul AG, Clifford S, Cioslowski J, Stefanov BB, Liu G, Liashenko A, Piskorz P, Komaromi I, Martin RL, Fox DJ, Keith T, Al-Laham MA, Peng CY, Nanayakkara A, Challacombe M, Gill PMW, Johnson B, Chen W, Wong MW, Gonzalez C, Pople JA (2005) Gaussian 03, Revision D.1. Gaussian Inc, Wallingford
- Alvira E, Mayoral JA, Garcia JI (1997) Chem Phys Lett 271:178–184
- Karelson M, Lobanov VS, Katritzky R (1996) Chem Rev 96:1027–1043
- Steiner T, Saenger W (1992) J Am Chem Soc 114:10146–10154
- Gejji SP, Taurian OE, Lunell S (1990) J Phys Chem 94:4449–4452
- Nakamoto K, Margoshes M, Rundle RE (1955) J Am Chem Soc 77:6480–6486
- Liu L, Song KS, Li XS, Guo QX (2001) J Incl Phenom Macrocycl Chem 40:35–39